MDPI

Review

Digital Pathology: A Comprehensive Review of Open-Source Histological Segmentation Software

Anna Maria Pavone [1,2], Antonino Giulio Giannone [3], Daniela Cabibi [3], Simona D'Aprile [2], Simona Denaro [2], Giuseppe Salvaggio [4], Rosalba Parenti [2], Anthony Yezzi [5] and Albert Comelli [1,6,*]

[1] Ri.MED Foundation, Via Bandiera 11, 90133 Palermo, Italy; ampavone@fondazionerimed.com
[2] Department of Biomedical and Biotechnological Sciences, University of Catania, 95123 Catania, Italy; simona.daprile@phd.unict.it (S.D.); simona.denaro@phd.unict.it (S.D.); parenti@unict.it (R.P.)
[3] Pathologic Anatomy Unit, Department of Health Promotion, Mother and Child Care, Internal Medicine and Medical Specialties, University of Palermo, 90127 Palermo, Italy; giulio.giannone@unipa.it (A.G.G.); cabibidaniela@virgilio.it (D.C.)
[4] Department of Biomedicine, Neuroscience and Advanced Diagnostics, University of Palermo, 90127 Palermo, Italy; p.salvaggio@libero.it
[5] Department of Electrical and Computer Engineering, Georgia Institute of Technology, Atlanta, GA 30332, USA; anthony.yezzi@ece.gatech.edu
[6] National Biodiversity Future Center (NBFC), 90133 Palermo, Italy
[*] Correspondence: acomelli@fondazionerimed.com

Abstract: In the era of digitalization, the biomedical sector has been affected by the spread of artificial intelligence. In recent years, the possibility of using deep and machine learning methods for clinical diagnostic and therapeutic interventions has been emerging as an essential resource for biomedical imaging. Digital pathology represents innovation in a clinical world that looks for faster and better-performing diagnostic methods, without losing the accuracy of current human-guided analyses. Indeed, artificial intelligence has played a key role in a wide variety of applications that require the analysis of a massive amount of data, including segmentation processes in medical imaging. In this context, artificial intelligence enables the improvement of image segmentation methods, moving towards the development of fully automated systems of analysis able to support pathologists in decision-making procedures. The aim of this review is to aid biologists and clinicians in discovering the most common segmentation open-source tools, including ImageJ (v. 1.54), CellProfiler (v. 4.2.5), Ilastik (v. 1.3.3) and QuPath (v. 0.4.3), along with their customized implementations. Additionally, the tools' role in the histological imaging field is explored further, suggesting potential application workflows. In conclusion, this review encompasses an examination of the most commonly segmented tissues and their analysis through open-source deep and machine learning tools.

Keywords: segmentation; digital pathology; deep learning; machine learning; open-source software; histological segmentation; WSI; histological images

1. Introduction

Biomedical imaging represents the key for the diagnosis and subsequent treatment of many pathologies, since it includes fundamental processes to obtain visible features about the human body. Hence, the aim of this research field is to support clinicians in more rapid and accurate diagnostic and therapeutic intervention processes [1]. In this context, artificial intelligence (AI) has played a key role in a broad variety of applications that involve the examination of a huge amount of data, including medical imaging [2–4]. Deep and machine learning, accompanied by pattern recognition tools, are developing into important components for extracting information that improve clinical diagnosis and predict disease progression [5]. Typically, AI is applied for the analysis of regions of interest (ROI) on a radiation therapy (RT) simulation scan, but also for computed tomography (CT), magnetic

resonance (MR)-guided RT, MR scans and other imaging techniques [6–9]. AI replaces some iterative analysis steps and enhances the efficiency and accuracy of the results [10,11]. In radiology and pathology fields, imaging experts support clinicians in order to recognize and detect lesion grading, highlighting specific features through mathematical filters [2,12,13]. In recent years, AI has also shown important results in the diagnosis and prognosis of emerging diseases, including COVID-19. In fact, several studies have been carried out to demonstrate the efficacy of AI-based diagnostic and prognostic models on CT medical images of COVID-19 patients [14–16].

Recently, the application of AI algorithms has been considered not only in the radiological area, but also in histopathology, giving rise to an emerging field of interest known as digital pathology [2,17–20]. Microscopic imaging still represents the gold standard for many bio-medical assessments [21–23]. In the era of precision medicine, digital pathology is a crucial tool in pathologists' daily activity, complementing their work rather than replacing it. In fact, the role of digital pathology is pivotal in addressing diagnostic challenges, providing unbiased and faster information that pathologists can leverage in decision making for a precise diagnosis, reducing the diagnostic variability [24–26].

First of all, the histopathological whole-slide images (WSIs) represent the supporting platform for the employment of AI algorithms and are derived by the acquisition and digitalization of tissue slides [27–29]. These last are obtained through laboratory steps, comprising paraffin-embedded tissues, sectioned into thin slices (of the order of μm), mounted on slides and stained [30–32]. Hence, digital pathology involves the acquisition, handling and interpretation of pathology knowledge, wherein image segmentation finds its broadest application [3,33,34]. This particular process consists of dividing images into several regions, in order to extract the features of interest. The criteria used are based on similar pixel information or intrinsic characteristics, including texture color and contrast. Thus, the images are separated into different groups, objects and background, which are decomposed in a meaningful way. This allows a more accurate analysis to be obtained and to take into consideration several features, including area, volume, shape, morphological irregularities, eliminating noise and weak edges issues [1,29,35–37].

While the segmentation process represents a great resource for digital pathology, on the other hand, segmentation has turned out to be one of the most pervasive issues in biomedical image analysis [38]. This explains the need to make segmentation an automatized and unbiased procedure, which may be utilized by users with low experience too. In order to solve the biological issue, researchers are working to develop innovative tools able to provide a fully automatic procedure [39]. However, images are currently processed through three different kinds of segmentation: manual, semi-automatic and fully automatic segmentation [40–42].

Manual measurements are applied in many areas of daily life: partitioning images are employed even in video surveillance, augmented reality or in the biomedical field, where tumor boundaries or tissue volumes are extracted, just to name a few applications [3].

In biomedical imaging, manual segmentation results are accurate, but extremely time-consuming. In fact, it sometimes takes several hours per patient, leading to critical delays in proceeding with RT treatment and impacting on the overall survival rate [40,43]. Also, the success of manual segmentation can be biased, since it is closely linked to the clinician's experience. For this reason, the introduction of semi-automatic or fully automatic segmentation methods has been necessary to enhance the achievement of better results [44].

Semi-automatic segmentation requires manual intervention, especially in the first steps of the procedure, while fully automatic procedures do not involve manual annotations. These methods provide expedients for high-throughput and quantitative investigations in digital pathology. Furthermore, assorted criteria of automatic or semi-automatic image segmentation include edge detection, threshold and Neural Network Image Segmentation [2,39,45].

Owing to the progression of digital pathology, several detection and classification tools have been suggested, such as for brain and breast tumor classification, and for the histopathological assessment of kidney tissue [46,47]. However, the full automatic seg-

mentation of histological WSI presents a challenge for many kinds of tissue, including liver and soft tissues, especially when the biospecimen structure is complex and heterogeneous [48,49]. The full characterization of histological tissues, especially for muscle and adipose ones, provides relevant information about the health status of the tissues. Indeed, morphological tissue modifications, such as anomalous fiber size distribution and aberrant plasticity, are important signals of onset disease that can be easily detected by digital pathology tools, which replace the time-consuming manual analyses [50]. In fact, some authors focused their studies on muscle and adipose tissue segmentation, implementing and customizing well-known open-source imaging tools, including ImageJ, as will be discussed in the next chapters [51].

To the best of our knowledge, not many reviews are focused on open-source segmentation tools applied on histological tissues. Therefore, the aim of this review is to investigate and to explore the emerging field of digital pathology and the most common open-source segmentation software employed, considering the last 10 years. Starting from the hundreds of articles found, exclusion and inclusion criteria were applied to obtain an optimal number of articles (about 180 articles available). Notably, we excluded proprietary software, customized algorithms and less used software. Instead, we have included the most used and intuitive software employed in histological segmentation. Some articles have been included in the introduction section, while the others focused on the in-depth application of software and were essential for the other sections of the review. It is worth noting that QuPath and Fiji are the most employed open-source software in digital pathology, among those taken into consideration (Scheme 1).
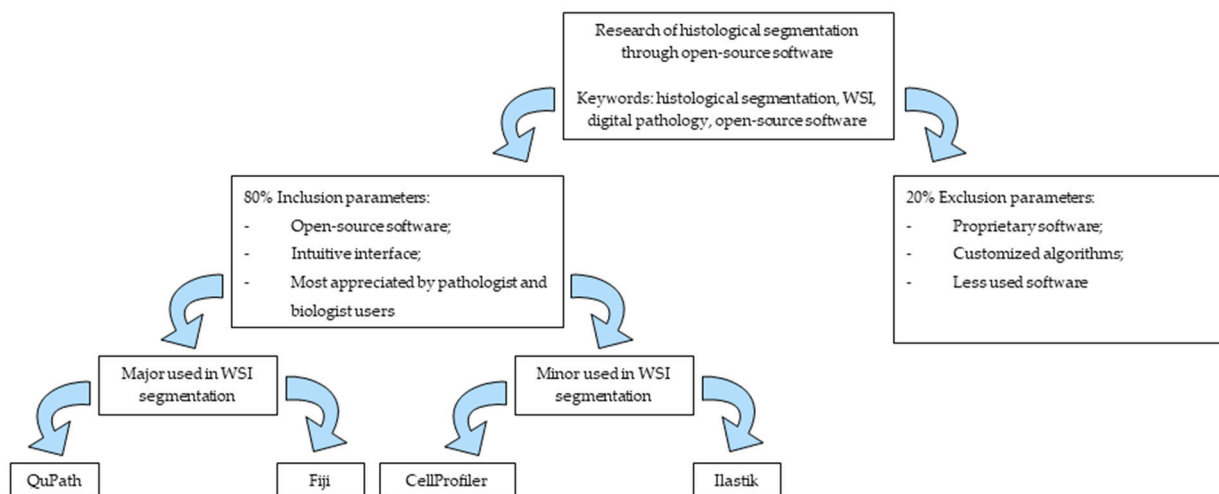
Scheme 1. Technical aspects of the review.

Specifically, this review comprises three main sections where we will summarize the main segmentation software applied in histopathology, different software workflows and the features of the most segmented histological tissues, in order to assist biologists and clinicians who want to explore this emerging field.

2. Software in Histological Segmentation

In recent years, the interest in digital pathology has been growing in order to overcome the impediments of visual analyses in histological tissues, through the acquisition of WSI, high-resolution images of histological sections obtained by tissue slides scans [52–54].

Recent advancements in hardware development have brought huge advantages for biomedical imaging. As aforementioned, segmentation, classification and detection methods represent the main applications of AI to digital pathology [1]. These segmentation techniques are not limited to whole-tissue analysis; they can also be applied to intracellular compartments, providing valuable quantitative insight into cell functions. Standard segmentation is based on edge recognition, threshold procedure, region growing and

morphology algorithms, and applied to nuclei detections, cell counts and cell type identification [1,55]. For instance, nuclear shape and texture can predict a patient's prognosis and recurrent risk in estrogen receptor (ER)-positive breast cancer patients [29].

In this context, the use of deep and machine learning is broadly required with a large amount of data, resulting in the need to develop innovative tools and software for this purpose [1]. The iterative training of AI algorithms is essential for automating cell and tissue segmentation, facilitating the analysis process [2]. These algorithms encompass pattern recognition, texture analysis and densitometry. Importantly, the algorithms need to be simple, intuitive and manageable, allowing beginner users to achieve their aims without practical issues [25]. In addition, these algorithms give rise to software solutions designed to discriminate tumor and healthy tissues, through manual and semi-automatic commands, showing data in a faster and more manageable manner. In this chapter, we will delve into four widely used open-source segmentation software including ImageJ, CellProfiler, Ilastik and QuPath, providing an overview of their main features and applications in histological imaging. Additionally, we will suggest specific workflows for each of these tools (Section 3). This may be useful to aid biologists and clinicians in performing and improving their analyses in the histopathological field [25].

2.1. ImageJ

ImageJ is open-source software widely adopted worldwide by biologists and pathologists in order to perform quantitative analyses. This analytical tool was presented by Wayne Raspband in 1997 and extended by several international groups of supporters, whose contribution plugins may sometimes be included in the main software source, giving rise to innovative versions and packages, including the well-known Fiji that consists of an innovative distribution of ImageJ [56–58].

ImageJ (v. 1.54) consists of an image-processing Java script that allows the user to visualize, edit and analyze 8, 16 and 32- bit images. Many versions are available for different operating systems, including Windows, Mac OS X and Linux, with the requirement of Java 1.4 or a later version installed. Moreover, different file formats are supported, including TIFF or raw data, as suggested at https://imagej.net/ij/index.html (accessed on 25 September 2023) (Table 1) [59].

The software are user friendly, with an intuitive interface that supplies several pipelines with many different functions [60]. In addition, ImageJ allows the development of customized pipelines to ease software activities based on the aim of analysis. In fact, some script modifications are performed to add new methods and types of analysis [56].

Although this software is used for many functions and data quantification, we will focus on its relevance in the histological segmentation field. The application of ImageJ to the histological field drove the researchers to focalize their activity on developing customized tools in order to analyze a particular tissue or histological section, through specific pipelines, in a simpler and more efficient manner. This is the case for MyoSight and AdipoSoft, which are specific for muscle and adipose tissue, respectively [61–63]. All these software and many others have the property of being able to take into account relevant features of each specific tissue, aiding the biologists and clinicians in the recognizing and analysis process.

ImageJ allows many other purposes to be achieved, including manual segmentation, through intuitive commands but also with semiautomatic plugins, such as Trainable Weka Segmentation [64,65], which aids the operator in performing accurate and faster segmentation. In fact, these machine learning algorithms can be trained to learn and repeat the same operation in new unknown data, called "test", and this is applied in order to simplify radiological diagnoses [66,67]. However, it is applied to histological segmentation, too [65]. In addition, manual segmentation can also be performed through the freehand selection tool in Fiji in order to trace accurate lineage around the moiety of interest, whose workflow will be explained in the next chapter [65].

In the paragraph below, we will show some examples of ImageJ/Fiji implementation in order to perform customized analyses for a specific tissue, such as muscle or adipose tissue.

Table 1. Summary table of ImageJ, CellProfiler, Ilastik and QuPath general information.

Software	ImageJ	CellProfiler	Ilastik	QuPath
Programming Language	Java	Python	Python	Java
Customized implementations	MyoSight, MyoSoft, MuscleJ, Adiposoft	Muscle Analyzer, Muscle2View	N/A	MyoSOTHES
Open Source	Yes	Yes	Yes	Yes
Download	https://imagej.nih.gov/ij/download.html (accessed on 25 September 2023)	https://cellprofiler.org/ (accessed on 25 September 2023)	https://www.ilastik.org/ (accessed on 25 September 2023)	https://qupath.readthedocs.io/en/0.4/docs/intro/installation.html (accessed on 25 September 2023)
Advantages	Possibility of developing customized plug-in; highly flexible functionality	High performance in detection of nuclei and cells in biological images	High performance in image segmentation	Intuitive interface Specific for histology and WSI analysis High performance in H&E images analyses
Limitations	Less specific for WSI	Specific for cell biology Difficulties in complex image analysis	Not specific for WSI Size limitations: object classifier training applied only in small images	Limits in plug-in customization

2.1.1. ImageJ Implementations

As mentioned above, ImageJ has been expanded by an international group of contributors and their customized plugins are useful when performing specific tissue analyses.

MyoSight, MuscleJ and MyoSoft represent the most common extensions for ImageJ/Fiji, in order to analyze histological muscle images through a semi-automated procedure [51,61,68]. Since these ImageJ implementations show similar proficiency in the histological imaging analyses, in this paragraph we will take MyoSight and Adiposoft as models of ImageJ implementation in muscle tissue and in adipose tissue, respectively. We will deal with MuscleJ (developed for Fiji version 1.51n) and other muscle software in Section 4.

MyoSight

MyoSight (for Fiji version 1.53c) is an ImageJ plugin and is downloadable at https://github.com/LyleBabcock/MyoSight, which contains the instruction manual, some test images and the application file, which requires the previous installation of ImageJ/Fiji [69].

The software was developed by algorithms able to identify muscle cell edges, using a combination of threshold parameters. Processing the histological sections through an immunofluorescence (IF) assay, such as a laminin staining, would be appropriate to mark the edges of muscle cells, in order to obtain a more careful and accurate segmentation [24,70]. However, no-staining images may be analyzed too. Indeed, the software allows for manual revision and correction of the segmentations in the case of automatic mistakes. The goal of imaging software should be the minimization of user input, but sometimes it is still necessary. MyoSight is employed for the analysis of cross-sectional area (CSA), the fiber-type distribution and nuclei detection, identifying the number of central and peripheral nuclei based on their position, since the nuclei position represents an essential element for determining damage in muscle tissue [68].

The identification of peripheral and central nuclei is facilitated by specific staining, including DAPI, a laboratory procedure that allows the blue staining of nuclei in IF images [71].

Adiposoft

Adiposoft is a fully automated open-source software developed with the purpose of performing adipose tissue analyses in histological slides. It is a plugin for Fiji, just like the software discussed previously. It is downloadable at http://imagej.net/Adiposoft (accessed on 25 September 2023), where many other information is available too [72]. As for the other ImageJ/Fiji plugins, the installation of Fiji is required to run Adiposoft.

Adiposoft allows the user to perform an accurate analysis of hematoxylin and eosin (H&E)-stained histological sections, especially in case of obesity, which is associated with an increase in the adipocyte number and expansion, hyperplasia and hypertrophy, respectively [62,73].

Adiposoft is often compared to AdipoCount, which is a free open-source software that performs a fully automatic segmentation, not developed by ImageJ and downloadable at http://www.csbio.sjtu.edu.cn/bioinf/AdipoCount/ (accessed on 25 September 2023) [74]. Adipocount is used for the ability to recognize and count the adipocytes present in histological images. In fact, it consists of three modules that allow membrane segmentation to be recognized, performing a re-segmentation and cell counting [62].

According to Xuhao Zhi et al., Adipocount outperforms Adiposoft in cell counting segmentation, since several cells are not well detected and counted by Adiposoft. However, Adipocount does not reveal area measurements and thresholding setting functions, contrary to ImageJ and its plugin [62]. For this reason, the better solution lies in combining methods, finding experimental settings that merge the strength points of AdipoCount and Adiposoft [40].

2.2. CellProfiler

CellProfiler is an open-source software whose first version was released in 2005 and was written in MATLAB. Over the years, more updated versions rewritten in Python have been released, up to the current version (CellProfiler v.4.2.6), which supports high-throughput 3D images analyses, already introduced in CellProfiler 3.0 [56,75]. In addition, since the combination of CellProfiler and ImageJ functions allows better results to be obtained, Lee Kamentsky et al. have developed a bridge to link CellProfiler pipelines to ImageJ plugins, since 2011 [76,77]. In addition, the CellProfiler source code and documentation are available at https://cellprofiler.org/ (accessed on 25 September 2023) [78]. The software is compatible with Windows, Mac and Linux operating systems, requiring Java installation before starting. Moreover, this open-source software supports a broad range of image formats, which are listed in the Bio-Formats library below https://docs.openmicroscopy.org/bio-formats/5.7.0/supported-formats.html (accessed on 25 September 2023) and that include even TIFF format (Table 1) [79,80].

CellProfiler represents a worthwhile resource in the biological field, since it allows an automatic segmentation to be performed with the feasibility to modify eventual software mistakes. In addition, after the segmentation process, the software allows the analysis of quantifiable cell measurements, such as CSA, centrally nucleated fibers (CNF) percentage and fiber size distribution, according to the shape, size, texture and intensity detection, providing morphological information, too [56]. These parameters are essential, especially in the skeletal muscle tissue analysis, as we will discuss in Section 4.

Like ImageJ, CellProfiler is open-source software that can be implemented by innovative pipelines, often customized for specific histological tissues. Among them, Muscle-Analyze and Muscle2View represent two CellProfiler-based pipelines suitable for skeletal muscle investigations [79]. Sharing the same interface as CellProfiler, MuscleAnalyzer allows measurements to be performed in less time than manual segmentation with a suitable application in skeletal muscle studies [71].

Regarding its performance, CellProfiler is designed to perform many image analyses at the same time, demonstrating its utility in high-throughput data investigations. Its reproducibility is also accompanied by analysis speed and accuracy, as demonstrated by Yeh Siang Lau et al., who performed a manual segmentation analysis of 67 muscle

histological images in about 3 h, while CellProfiler took about 11 min to complete the same analysis, proving its superior efficiency [56,71].

The organization of CellProfiler consists of modules that allow the user to access different kinds of functionalities. In the manual, all these functions are explained in an easy-to-understand manner in order to assist the beginners, and a community has also been created to provide assistance and answers to the user's questions [56,77].

2.3. Ilastik

Ilastik (v. 1.3.3) is open-source software written in Python and operating in image analysis. It is available for Windows, Mac and Linux and requires a 64-bit system and at least 8 GB of RAM, with more RAM recommended for 3D images [81]. The free software is downloadable at https://www.ilastik.org/ (accessed on 25 September 2023) where the manual is available too, in order to guide the beginner user's first steps (Table 1) [82]. Ilastik supports many formats that are listed on https://www.ilastik.org/documentation/basics/dataselection#formats (accessed on 25 September 2023) [83].

This software allows different imaging analyses to be made, such as an evaluation of pixel intensity, a classification of objects, density counting, thresholding procedures and size filters. All these functions are tightly connected to the segmentation process, which can be applied to microscopic images derived from cell culture or histological tissue [81].

In the first case, Ilastik is able to perform organelle segmentations, especially mitochondrial assessment, as described by Christian A. Fischer et al., in HeLa cell culture [84]. These segmentations showed that the average mitochondrial area was larger in untreated cells, compared to HeLa cells treated with oligomycin and antimycin. However, Ilastik does not achieve the results of other specific software, such as MitoSegNet 1.0 [84]. Although Ilastik is not specific for WSI analysis, researchers apply this software in order to analyze histological images, too. This is the case for Sharon C. Yates et al., who demonstrated the possibility of applying Ilastik segmentation to rodent brain tissues previously subjected to immunohistochemistry (IHC) staining [85]. Ilastik also allows image processing, distinguishing the background from the objects, counting the objects of interest, evaluating the pixel intensity, nuclei segmentation and training images. This latter analysis is due to the machine learning approach of this software. However, the object classifier can be trained only in small images, including tiles of WSI. For this reason, this software is not very often used in WSI analyses. However, the high throughput Ilastik tile segmentation has been shown to be accurate, compared with manual segmentation and other software, including Quint, developed for quantification and spatial analysis for high throughput investigations [84,86].

2.4. QuPath

Quantitative PAThology (QuPath) is open-source software written in Java whose 0.4.4 version is available at https://qupath.readthedocs.io/en/0.4/ (accessed on 25 September 2023) [87,88]. It supports many formats, like the other above-mentioned software, which are listed at https://qupath.readthedocs.io/en/0.4/docs/intro/formats.html (accessed on 25 September 2023) (Table 1) [89].

QuPath exploits deep learning in order to become one of the most used tools in the field of histological segmentation. Unlike the previously mentioned software, which can also perform other types of analyses, QuPath was primarily developed to assist pathologists in the diagnostic process. Its intuitive interface is especially useful when working with WSI and a large amount of 2D data [87,88,90].

The functionalities of QuPath applied to histological sections are multiple: in fact, it allows annotations, training classifications and cell and nuclei identifications to be performed. In this context, QuPath represents a valid alternative to CellProfiler and Fiji for nuclei detections in the histological field, especially for cancer diagnosis [91]. In order to attest to the software's accuracy, QuPath segmentation has been compared to manual

practices in different conditions, including in breast cancer, where QuPath segmentation analyses had similar results to the manual segmentation assessments [92].

QuPath is "object-based" software, in which an object consists of a region or an element that can be individuated and segmented into the image. Moreover, the objects can be classified and related each other, and are called object "parent" and object "child". This is the case in nuclei and cell classifications, which are often related to improve the analysis results [87].

The automatic nuclei segmentation can be easily performed by H&E staining, without the need for ancillary techniques such as IF and IHC. This is an advantage, since H&E staining is a low-cost and quick procedure which is routinely used for histological diagnosis [91,93]. Further, QuPath is applied in many different research areas, such as nephrology, neurology and oncology, as we will discuss in Section 4.

QuPath Extension: MyoSOTHES

Not many QuPath plug-ins have been implemented over the years. Marie Reinbigler et al. developed a new software called MyoSOTHES, derived from the combination of QuPath and CellPose, another deep learning-based segmentation tool [94].

MyoSOTHES (Myofibers Segmentation wOrkflow Tuned for H&E Staining) allows the performance of automatic segmentation applied to muscle fibers and it was tested on groups of 50 mice affected by Sarcoglycanopathy, in order to evaluate the phenotypical effects of the proposed treatment on the fibers [94,95]. In this case, MyoSOTHES was compared with CellPose and QuPath, reporting promising results. In fact, fiber damage has been detected through segmentation analyses, highlighting the peripheral location of the nuclei in the muscle fibers and the high CNF ratio, which are indicators of anomalies in muscle tissue [94].

MyoSOTHES is accessible from Windows, Mac and Linux, with low requirements including 2 GB of RAM and 2 GB of GPU. However, there are not so many studies related to the usage of this software.

## 3. Proposed Workflows

3.1. Tissue Preparation

Tissues need to undergo processing before being analyzed, whether they are human or mouse tissue. In the case of a mouse or rat model, tissues are collected after animal sacrifice. The organs are fixed in paraformaldehyde (PFA) 4% or formalin, and then processed through paraffin or Optimal Cutting Temperature (OCT) embedding, cut and mounted on slides, according to traditional protocols [73,92] (Figure 1).

3.2. Staining Process

The importance of the staining process resides in highlighting the structures and elements needed for the analysis (Figure 1). WSIs are usually acquired in brightfield, after a H&E staining [96,97]. This staining is important for the characterization of tissue morphology, although it lacks cell-related molecular information. However, biomarker detection is possible through immunolabeling processes, including IF or IHC. These techniques are employed to distinguish cell types, characterizing predictive and diagnostic biomarkers [24,70].

Furthermore, in IF, DAPI staining is essential to perform nuclei detection, since this technique allows the presence of nuclei to be highlighted through blue coloration [71].
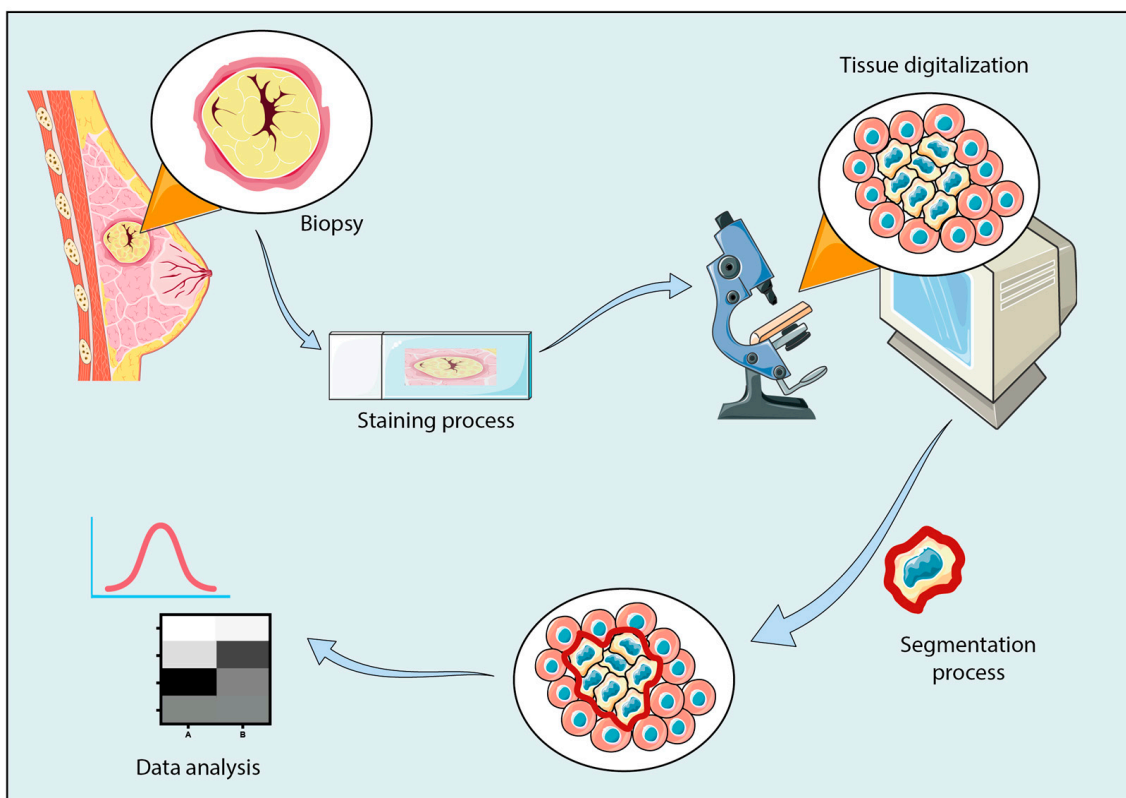
Figure 1. Representative workflow of the histological segmentation process. After tumor detection, a biopsy is performed and processed through paraffin or OCT embedding, cutting process and slide montage. The slide is stained with specific procedures and observed through the microscope. Through the digitalization process, the visualization of histological tissue and the use of segmentation software are allowed, in order to analyze the histological sample by segmentation. Then, data analyses are performed to obtain diagnostic results.

3.3. Image Acquisition and Dataset

Tissue digitalization may be performed by capturing WSIs through many kinds of scanners, which allows images to be acquired with different parameters, including size and illumination, and to be saved in many file formats (Figure 1). Using the same file format assures a more homogeneous and reproducible analysis. In radiology, the widespread image format is represented by DICOM, which allows examination and access to a large amount of image data. Digital pathology has not adopted a unique file format yet, even if the progress is moving towards that direction [70]. However, according to the biomedical applications, the TIFF format represents one of the most common image formats used to perform histological segmentation imaging, for easier image processing, although many of the previously mentioned software also support JPEG, PNG, SVS and other formats [98]. In fact, the TIFF format is able to support a large amount of data and it proved to be worthwhile in high throughput analyses [53].

In addition, the capture process is fundamental for the success of analysis. Usually, clinicians observe the WSI at $5\times$ magnification, in order to survey the potential tissue alterations. Then, these findings are analyzed using major magnification, including $20\times$ or $40\times$ [93].

Another important aspect of the acquisition is the field of view (FOV), which varies based on the magnification and the optical system. According to Robert Paulik at al., a standard microscopic FOV may be around 1–1.5 mm^2 for $20\times$ magnification images and 0.2–0.3 mm^2 for a $40\times$ magnification setting [99].

3.4. Proposed Software Workflows

3.4.1. ImageJ/Fiji—Proposed Workflow

Assuming the necessity to segment muscle tissue images, following laminin staining after the importation of images on ImageJ/Fiji, we propose some commands that may be useful to perform manual segmentation analysis, according to Jenna M. Kastenschmidt et al.:

- Make binary: allows the conversion to binary images.
- Wand Tool: allows the operator to design the edges of myofibers.
- Measure function: allows the calculation of the area (μm^2), the minimum Feret diameter (μm) and all the measurements that the analysis requires.

In addition, an important step during imaging analysis is the setting scale. In order to realize this step, we suggest loading an image containing a known linear scale bar. In this way, it is possible to set the scale drawing as a line overlapping the scale bar of the image.

The set scale option is used to set the known distance: if the ratio is 1:1, the "pixel aspect ratio" is required to be 1 and the "Known Distance" parameter needs to be completed, inserting the known distance. Clearly, the measurement unit depends on the scale bar (i.e., μm).

Finally, the "Global" preference assures the maintenance of the setting for all following images, considering all the images with the same magnification [100].

3.4.2. CellProfiler—Proposed Workflow

The many modules provided by CellProfiler allow the user to achieve the set goals. According to Yeh Siang Lau et al. and assuming the need to analyze muscle section IF images, after laminin and DAPI staining, we will discuss the most used modules in the segmentation process [71,92]:

- In order to perform muscle fiber analysis:

Muscle fibers can be identified through the Identify Primary Objects Module, filtering the diameter of fibers in order to exclude every object out of the diameter range. Then, the threshold may be applied through the Robust Background Module, adjusting the parameters and including the threshold and size of the smoothing filter, to obtain a more accurate fiber identification.

In case of IF staining, the Measure Object Intensity Module is suitable to detect the intensity of fluorescence and the Measure Object Size Shape Module allows the total muscle fiber number and area of segmented moieties to be obtained [92].

- In order to identify nuclei and their position:

The Identify Primary Objects Module may be used to identify the nuclei stained with DAPI, taking into account the previously mentioned parameters, and the Expand Or Shrink Object Module may be used to perform a more accurate nuclei classification, discriminating central nuclei from the de-centered ones. The ratio between central nuclei fibers and lateral nuclei fibers is important in many pathological conditions, as we will discuss in Section 4. For this purpose, the Relate Objects Module is a valid alternative to the manual count. This function allows two objects to be related: the first object will be the "child object", which is represented by the number of nuclei; the second one is the "parent object", which represents the number of fibers in the case under consideration. It is useful to count the number of nuclei associated with the muscle fibers.

Then, the Classify Objects Module allows the fiber containing central nuclei to be distinguished from the others [71].

3.4.3. Ilastik—Proposed Workflow

The Ilastik segmentation workflow is congruent with segmentation performed by other software, including ImageJ [85].

Assuming the need to segment IHC-stained images, the Pixel Quantification module is essential to discriminate the immunoreactive moiety from the background. This module takes into account all the accessible features, including the intensity of the pixel, texture and edge. The first image analyses are performed as training, in order to apply the annotations to the whole image dataset.

After the Pixel Quantification phase, the Object Quantification can aid the user to differentiate the immunoreactivity from artefacts that may disrupt the signal. This classification is carried out by filtering the objects according to their features, such as shape and size. Then, the trained classifier has to be applied to the total image set.

This workflow allowed Yates et al. to complete segmentation analyses with 95% confidence within 0.32% of error, compared to other segmentation methods for an image series consisting of immunostained brain tissue images [85].

3.4.4. QuPath—Proposed Workflow

According to Paola S. Apoulauza et al., who used QuPath for pancreas histological analyses, we propose a general workflow for using QuPath [101].

Assuming the need to perform IHC-stained segmentation analyses, the first step consists of carrying out a Pixel classifier in order to obtain tissue detection, exploiting the intensity thresholder functionality.

The object detection is performed through Pixel classification and training Pixel classification processes that let QuPath be trained to discriminate between different kinds of objects (or cells).

Finally, the cell detection procedure is performed through the cell detection command, followed by the nucleous threshold, segmentation and the addition of smoothed features, which allows only objects within a specific measure (i.e., 25 μm, according to the kinds of analyses and dataset) to be taken into account.

Then, annotations can be exported as an CSV file to be processed using Excel (Figure 1).

4. Histological Tissue Segmentation

Digital pathology represents an important resource for clinicians who need to obtain answers about biopsy tissues in a very short time. Thus, the use of AI is also useful for biologists and other researchers who have large amounts of data to analyze [70] (Figure 1).

In this chapter, we will focus on the most segmented histological tissues, taking into account the tools and methods used to perform these kinds of analyses.

Although the previously reported software are the most used in digital pathology, many other segmentation tools have been developed for this purpose, exploiting the proper features of each tissue. It is challenging to determine which of these methods performs best in segmentation analyses. Thus, we decided to carry out a brief excursus of the most common segmentation tools applied in the tissues of interest.

4.1. Skeletal Muscle Tissue

Skeletal muscle is a high complex tissue, organized in bundle of fibers called myofibers. Each of these constitutes a muscle cell whose functional unit is represented by the sarcomere. Myofibers are organized in fascicles, forming muscle tissue that is enveloped by connective tissue. The maintaining of this organization is essential to the preservation of the physiological functions in muscle tissue. In fact, little perturbations of this balance may lead to the loss of muscle health, followed by the onset of severe pathological conditions [102,103].

Among the myopathy disorders, an example is represented by Duchenne muscular dystrophy (DMD), which is a severe dystrophinopathy due to the deficit of dystrophin expression, caused by genetic mutations and followed by sarcomere strains and sarcolemma tears [104–106]. In order to study this X-linked fatal myopathy, dystrophin deficient mice, including a muscular dystrophy X-linked (mdx) mouse model, are enrolled in preclinical research. Owing to this model, many studies have been focused on the continuous cycle of

muscle injury and regeneration, which leads to an increasing heterogeneity in myofiber size and organization, also associated with central nuclei localization. On the other hand, Wild Type mice show a uniform myofiber size and distribution [61,68,107]. In particular, according to Alicia Mayeuf-Louchart et al., in a dataset of injured and healthy skeletal muscle images, MuscleJ analyses revealed that only about the 4% of fibers showed central nuclei in controls, against about 58% in injured muscles. The results are compatible with manual segmentation analyses undertaken by five experts [61]. These injury muscle features are confirmed by many other studies, using different dataset and segmentation software, developed with the purpose of facilitating the myofiber segmentation and the following measurements. This is the case for MyoVision, which is an approved software to assess the CSA, myofiber type and myonuclei detection. However, it does not analyze the CNF parameters, contrary to QuantiMus, a machine learning-based tool that was developed for this purpose. In fact, it integrates the analytical characteristics of previous software, including the ability to calculate fluorescence intensity in myofibers [100]. Moreover, in the field of sarcoglucanopathies, a fully automated software called MyoSOTHES was developed in order to analyze large amounts of WSI data. In this case, the investigation was performed in H&E images, carrying out a deep study through phenotype indicators such as CNF ratio and Feret's diameter measurements [94].

All this software often need to be associated with the preprocessing of the sample, which consists of highlighting specific characteristics through staining processes. Among them, the myosin heavy chain (MyHC) is useful to discriminate the fiber types and Laminin α2 represents an effective method to recognize the myofiber edges. This preprocessing aids the automatic software to discriminate the objects of interest from the background [64,71]. In addition, DAPI staining is strictly recommended for nuclei detection, as suggested in Section 3.

Although many preclinical studies have been performed in relation to mdx mice, clinical research is progressing in this field, too. In fact, recent studies have been performed in human patients. This is the case for Perla C. Reyes-Fernandez et al., who have developed an innovative, fully automated macro in Fiji in order to perform an automatic detection of myofibers in slides of muscle deltoid biopsies derived from patients with dermatomyositis (DM), necrotizing autoimmune myopathy (NAM) and anti-synthetase myopathy (ASM) [108].

4.2. Renal Tissue

Kidneys are paired organs localized in the retroperitoneum that play important role in excretory functions, maintaining the homeostasis of extracellular fluids [109,110]. Indeed, their main function involves blood ultrafiltration, with the consequent production of urine, useful for the preservation of metabolites, ions and water balance. This role is played by renal glomeruli, which are located on the renal cortex and provide the ultrafiltration of capillary blood. Aberrations at glomeruli levels may lead to serious diseases, causing potential renal failure and cardiovascular dysfunctions. Thus, the prompt recognition of renal dysfunctions and morphological irregularities may be an important resource to avoid severe physiopathological conditions [111].

In the overall context, even in this field the need to find innovative methods is emerging to improve and accelerate diagnoses, owing to AI approaches.

The most used deep learning method applied to digital pathology consists of the employment of convolutional neural networks (CNN), owing to their notable performance in several analyses, such as histology segmentation and nuclei detection. In particular, deep and machine learning methods are often applied to the detection and segmentation of glomeruli in WSIs of kidney slices [90]. While the initial application of CNN merely regarded the segmentation of glomeruli, to date CNN applications have also been extended to other parts of the kidney, such as tubuli and interstitium, investigating both healthy and pathological tissues and showing glomerular size variability, interstitial and tubular expansion and atrophy in aberrant tissue [47,90]. In this context, two algorithms have been

developed, known as RENFAST (Rapid Evaluation of Fibrosis And vessels Thickness) and RENTAG (Robust Evaluation of Tubular Atrophy and Glomerulosclerosis). RENFAST is designed for detecting vessels and interstitial fibrosis, while RENTAG focuses on detecting and classifying glomeruli and tubules [112,113]. Other researchers have also introduced similar semantic segmentation CNN models, albeit with slight variations. These models were trained on relatively small datasets of pre-implantation kidney biopsies stained with Periodic Acid-Schiff (PAS). They were initially utilized for the detection of vessel and tubular structures, employing binary classifier classifications. Further progress has been made by incorporating the use of Local Binary Pattern (LBP) and Haralick features, which enabled the consideration of a wider range of features. However, the most notable advancements were made through the utilization of models based on SegNet and DeepLab networks [113].

Consequently, the accurate classification of glomerular conditions holds significant importance in the diagnosis of various kidney ailments. Moreover, these models have proven instrumental in the domain of transplant kidney biopsies, facilitating the detection of organ quality, the prediction of rejection risks and the diagnosis of other related conditions [112,114]. Many other CNN algorithms are applied in kidney histological investigations, such as U-Net algorithms that were shown to be particularly relevant for segmentation processes [115–118]. U-Net training can be supported by other software, including QuPath. As shown by Nassim Bouteldja et al., QuPath software can be used to perform segmentation and pre-annotations, reducing the need for a manual annotation process. Also, the QuPath support in the annotation process accelerated the training phase of U-Net. The annotations have been supervised by expert nephrologists [90,119].

Furthermore, a total open-source approach provides for the combination of Ilastik and ImageJ software in order to perform an automatic segmentation procedure, followed by digital image measurements. Indeed, this software provides the skill to analyze multiple images at the same time, allowing batches of images to be processed at once. Susan M. Sheehan et al. have applied this approach on human tissue, through the analyses of 121 images derived from 12 patients, obtaining promising results although the detection of many false positive cases, probably due to the poor visibility of the nuclei in the tissue [120].

4.3. Cancer Tissue

The recognition of cancer tissue represents one of the most frequent activities for pathologists. However, the identification of subtle neoplastic changes can be challenging; in this setting, the use of digital pathology may be helpful. Owing to the advent of digital pathology, this process has undergone many improvements, leading to a widespread use of deep and machine learning methods for segmentation processing [121].

Many studies have been carried out to develop innovative pipelines and tools in order to analyze and distinguish healthy from cancerous tissue.

4.3.1. Breast Cancer

Breast cancer is one of the most pervasive tumors in women, associated with a different rate of overall survival based on the kind of tumor and a timely diagnosis. In fact, early diagnosis represents the essential element to ameliorate patients' prognosis and it is encouraged to prevention screening through mammography and ultrasound imaging, following by a biopsy of breast tissue in the case of suspected cancer advance [122–124]. Then, the crucial role of the pathologist consists of the prompt recognition of the tumor tissue, also assisted by specific biomarkers, including ER, the type-2 epidermal growth factor receptor (HER2) and the progesterone receptor (PR), which characterize the type of breast neoplasm. In combination, other biomarkers of prognostic and therapeutic interest, such as Ki-67, provide an indication about the proliferation rate of tumor cells [99,124–126].

Therefore, classifications into benign and malignant tissue results are extremely important for the diagnosis and are often performed through manual segmentation, a time-consuming practice performed by expert pathologists [124]. Some semi-automatic approaches allow classification to be performed, aiding the clinician in the segmentation

process. The pixel classifier of QuPath was applied to H&E breast cancer images in order to segment the tumor epithelium, stroma and fat tissue [127]. This approach was also applied in a preclinical xenografted mouse model, where cell classification was performed using a combination of Fiji and QuPath functionalities [128]. Fiji, in particular, has also been employed for pixel classification and the detection of brain metastasis of breast cancer [129].

Although digital pathology has not been widely adopted in clinical practice, some pathologists have shown interest in semi-automatic or fully automatic approaches. This is the case for Lieze Berben et al., who carried out studies about the characterization of immune infiltrates in breast cancer, confirming the accurate method analyses of the aforementioned software, QuPath. The validation of this software was also performed through manual counting, showing promising results. In fact, following the staining of positive and negative lymphocytes, QuPath analysis revealed a correct identification of the evaluated markers, such as CD8 and CD20, with a little overestimation of negative stained immune cells. However, regarding the other parameters taken into consideration, the positively stained immune cell evaluation did not show relevant differences between manual and QuPath counting; rather, a tight correlation was observed in the results of the assessed protocols [130].

4.3.2. Glioblastoma

Glioblastoma (GBM) is an aggressive tumor, composed by complex heterogeneity features that make personalized therapeutic approaches difficult, leading to an overall survival of 15–18 months [131,132]. Moreover, GBM is characterized by a hypoxic microenvironment that is related to the reduced efficacy of therapies and leading to a probable relapse with poor prognosis [133]. Digital pathology may provide valuable support to GBM diagnosis, although only a limited number of software have been employed for this purpose. Among them, QuPath was used for cell segmentation, classification and staining quantification in histological slides of GBM [134].

An interesting study was conducted by Valentina Brancato et al., who investigated the potential cross-talk between radiomic and pathomic features in GBM patients. Hence, the authors established correlations between radiomic features obtained from functional MR images and histological features extracted from H&E tissue slides. These studies focused on key radiomic features in MR, such as Apparent Diffusion Coefficient (ADC), which is considered a biomarker for estimating cellularity. This radiomic biomarker was compared with pathomic features, including nuclei count. The investigations showed an inverse correlation between ADC and nuclei counts, along with a positive correlation between ADC and extracellular space, confirming previous studies [135,136]. In order to perform these analyses, QuPath and PyRadiomics have been employed for pathomics and radiomics extraction, respectively. In particular, a QuPath implementation script was used to carry out nuclei segmentation and the extraction of features. In addition, annotations have been performed in relation to the WSI area and nuclei identification [135].

Beyond QuPath, other software has been applied to histological segmentation in GBM. In this context, PathoFusion is open-source software for the identification of morphological signatures in pathological tissues. In particular, Alzoubi et al. highlighted the PathoFusion role in the WSI patch classification and segmentation of individual GBM cells [55]. However, other GBM studies demonstrated that PathoFusion may offer a relevant aid to train CNNs in recognition of pathological conditions in histological slides [137].

4.3.3. Colorectal Cancer

Colorectal cancer (CRC) still represents a cause of death worldwide, in which early detection and grade identification represent an opportunity to improve overall survival [13,138,139]. Early diagnosis is supported by the exploitation of specific biomarkers associated with radiological imaging analyses. Thus, several authors have proposed prognostic prediction models through tumor segmentation, which has reported a more significant analysis than the model without tumor segmentation [139,140]. Relevant studies have been carried out,

employing CellProfiler and QuPath for the nuclei classification of colorectal cancer slides, showing promising results [52]. QuPath was also used to train H-DAB images, exploiting the ability to create annotations to classify the different ROIs of the tumor slide [141].

Moreover, other studies have been carried out using QuPath as a manual annotation tool in the analyses of 312 H&E stained histological sections belonging to patients with second stage colon cancer. In this context, the open-source software was associated with scripts able to automatize the background identification and the intensity of image channels, which were different according to the scanner used. This standardization plays an important role in imaging analyses [87]. It is an essential process for the analysis reproducibility. In fact, standardization is relevant for preserving the quality and integrity of image data, minimizing the impact of noise, artifacts and errors [142].

QuPath was employed to perform an SLIC superpixel segmentation, a procedure that generates superpixels. In particular, the combination of this procedure with the "Add intensity features" and the "Add smoothed features" QuPath commands allows a multitude of information about the tissue to be accessed and the classification process to be ameliorated [87]. In addition, QuPath can be also used as training software. This is the case for et al.'s study on WSI images of colorectal cancer, stained with hematoxylin and DAB.

5. Discussion

In the era of precision medicine, digital pathology plays a pivotal role in addressing diagnostic challenges by providing faster and more accurate information. Pathologists can leverage this information in decision-making for a precise diagnosis, thereby reducing the diagnostic variability.

In this context, we have identified the most used open-source segmentation software, including ImageJ, QuPath, Ilastik and CellProfiler, able to perform the most requested analyses in digital pathology (Table 2).

Comprehension of the mentioned software, combined with the propensity to employ these tools, is essential in advancing digital pathology progress, a goal that this review aims to achieve. The innovation of this review consists of the distinctive contribution to the rising knowledge in digital pathology and the potential applications within this emerging field. In addition, this review is designed to serve as a resource for newcomers to this area, leading them through workflows and illustrating functionalities applicable to different tissues.

In the diagnostic field, all the mentioned software provide relevant advantages compared to manual image analysis, which is highly labor-intensive and liable to variability [71,85,101,143].

According to our research, Fiji emerges as the predominant open-source software in image analysis. Notably, the other mentioned software have Fiji plugins, aiding analysis combinations. Fiji is versatile software that carries out different kinds of image analyses compared to QuPath, which is specifically designed for WSI and histological analysis. QuPath is more intuitive for pathologists compared to the other software, including Ilastik, CellProfiler and the broader functionality of Fiji. In fact, they lack specific functions developed for WSI [141].

On the other hand, Fiji excels in flexibility, allowing the users to develop specific plug-in, as in the case for MuscleJ, MyoSight, MyoSoft and the other plug-in aforementioned in the review [23,34,41].

CellProfiler and Ilastik are less commonly employed for WSI. Notably, Ilastik is not specifically designed for WSI, but boasts different functionalities, enabling the user to evaluate local signals including light, colors and structure of images [81]. Its versatility extends to cell segmentation, thereby assisting in the annotation process. Consequently, Ilastik finds applicability across various imaging field, including histological analysis [144,145]. Conversely, CellProfiler is tailored towards the specific task of identifying and quantifying cells and nuclei [91,98]. This software offers clinicians and biologists a relevant aid in obtaining extensive phenotypic data related to the shape, size and counts of cells [146] (Table 2).

Table 2. Recent advancements in ImageJ, CellProfiler, QuPath and Ilastik implementations.

Software	Plug-in	Tissues	Image (WSI or ROI)	Main Analyses	References
ImageJ/Fiji	Fiji and WEKA plugin	Kidney, Muscle, Breast, Brain metastasis	ROI and WSI	Object quantification; Nuclei segmentation; Detection of brain metastasis; Cell classification;	[77,91,120, 128,129]
	BoneJ	Bone.	ROI	Measurement of osteoclast area and trabecular thickness.	[63]
	AdipoCount	Adipose tissue	ROI	Adipocytes quantification	[62]
	MuscleJ MyoSight MyoSoft	Muscle	ROI	CSA; Fiber quantification and distribution; Myonuclei localization and quantification.	[51,61,68]
CellProfiler	MuscleAnalyzer Muscle2View	Muscle	ROI	CSA; Fiber quantification and distribution; Myonuclei localization and quantification.	[71,79]
	CellProfiler	Muscle, Gastrointestinal, Colorectal cancer.	ROI	Object detection and classification; Nuclei segmentation and classification; Quantification of muscle parameters; Cell segmentation.	[52,77,91, 92,107]
QuPath	MyoSOTH	Muscle	ROI	CSA; Myonuclei localization; CNF ratio.	[94]
		Muscle, Kidney, Brain, Cancer tissues: Breast, GBM, Liver, pancreatic, colorectal.	ROI and WSI	Object detection and classification; Nuclei segmentation and classification; Cell segmentation; Staining quantification.	[90,91,101, 119,128,130, 134,141]
Ilastik		Gastrointestinal; Brain; Kidney.	ROI	Object detection and classification; Counting and tracking; Cell Segmentation; Training classifier.	[85,92,120]

To the best of our knowledge, not many reviews focused on the comprehensive comparison of these software, excepted for a limited number of studies that have employed a broader spectrum of software options [52,77,85,91].

However, comparing software used in different studies represents a great challenge. One of the main limitations of digital pathology consists of the poorly standardized processes of acquisition and pre-acquisition, leading to limited analysis reproducibility. The lack of image and parameter standardization hinders meaningful comparisons between different tools. In fact, digital pathology is still far from being used in the daily clinical routine [54,147].

Thus, this review aims to address these gaps by providing a thorough exploration of various software platforms and presenting several application examples. The goal is to provide a wide range of information about these software options, enabling the users to make informed decisions based on their specific needs.

6. Conclusions

Digital pathology represents an innovative method of analysis for pathologists and clinicians. The importance of this area is dictated by the necessity of finding faster and

more effective procedures to make diagnostic and therapeutic areas more accessible and productive [2,3,33,54].

In this context, segmentation represents an essential process in imaging analyses. The latter procedure allows for the individuation and definition of a specific ROI to analyze. Already used in radiological and other medical applications, segmentation is taking hold in digital pathology as well, through the introduction of a series of open-source software able to aid in the analyses through semi-automatic or fully automatic segmentation methods, improving the time-consuming manual process and allowing large amounts of data to be analyzed in high-throughput investigations [40,43].

Aware that machine and deep learning algorithms have already been employed in the biomedical field for years, in this review we have summarized the most common open-source segmentation software, including ImageJ, CellProfiler, Ilastik and QuPath, in order to aid clinicians and biologists with their segmentation analyses, as well as providing workflow methods of analyses. In fact, this software allow many purposes such as edge and nuclei detection, thresholding process and CSA measurements to be achieved in a faster and more intuitive way than in the past [1].

Given the promising results of the currently used software, the future direction looks to the development of innovative, fully automatic tools which will support the clinicians' decision-making, reducing inter- and intra- operator variability and ensure the reproducibility of the results through unbiased procedures. The pathologists maintain their crucial role and will be involved in the development of innovative workflows, aiding the standardization processes.

Currently, digital pathology is still far from clinical application. However, given its fast spread, the expectation is that the guidelines for pathologists' practice may move towards standardization in the near future. This process will pave the way for a new era of digital pathology in clinical practice.

Until that moment, the use of open-source software emerges as an optimal choice to perform histological analyses, in order to develop crucial skills in this emerging area, which may become a valuable resource in the coming years.

Institutional Review Board Statement: Not applicable.

Informed Consent Statement: Not applicable.

Data Availability Statement: Not applicable.

Conflicts of Interest: The authors declare no conflicts of interest.

Abbreviations

AI	artificial intelligence
CT	computed tomography
MR	magnetic resonance
ROI	region of interest
WSI	whole-slide images
CSA	cross-sectional area
H&E	hematoxylin and eosin
CNF	centrally nucleated fibers
DMD	Duchenne muscular dystrophy
Mdx	muscular dystrophy X-linked
MyHC	myosin heavy chain
DM	dermatomyositis
NAM	necrotizing autoimmune myopathy
ASM	anti-synthetase myopathy
CNN	convolutional neural networks
RENFAST	rapid evaluation of fibrosis and vessel thickness
RENTAG	robust evaluation of tubular atrophy and glomerulosclerosis
GBM	glioblastoma
ADC	apparent diffusion coefficient
CRC	colorectal cancer
IF	immunofluorescence
IHC	immunohistochemistry

References

1. Anwar, S.M.; Majid, M.; Qayyum, A.; Awais, M.; Alnowami, M.; Khan, M.K. Medical Image Analysis Using Convolutional Neural Networks: A Review. *J. Med. Syst.* **2018**, *42*, 226. [CrossRef]
2. Durkee, M.S.; Abraham, R.; Clark, M.R.; Giger, M.L. Artificial Intelligence and Cellular Segmentation in Tissue Microscopy Images. *Am. J. Pathol.* **2021**, *191*, 1693–1701. [CrossRef]
3. Minaee, S.; Boykov, Y.; Porikli, F.; Plaza, A.; Kehtarnavaz, N.; Terzopoulos, D. Image Segmentation Using Deep Learning: A Survey. *IEEE Trans. Pattern Anal. Mach. Intell.* **2022**, *44*, 3523–3542. [CrossRef]
4. Scavuzzo, A.; Pasini, G.; Crescio, E.; Jimenez-Rios, M.A.; Figueroa-Rodriguez, P.; Comelli, A.; Russo, G.; Vazquez, I.C.; Araiza, S.M.; Ortiz, D.G.; et al. Radiomics Analyses to Predict Histopathology in Patients with Metastatic Testicular Germ Cell Tumors before Post-Chemotherapy Retroperitoneal Lymph Node Dissection. *J. Imaging* **2023**, *9*, 213. [CrossRef]
5. Alongi, P.; Stefano, A.; Comelli, A.; Spataro, A.; Formica, G.; Laudicella, R.; Lanzafame, H.; Panasiti, F.; Longo, C.; Midiri, F.; et al. Artificial Intelligence Applications on Restaging [^{18}F]FDG PET/CT in Metastatic Colorectal Cancer: A Preliminary Report of Morpho-Functional Radiomics Classification for Prediction of Disease Outcome. *Appl. Sci.* **2022**, *12*, 2941. [CrossRef]
6. Kim, H.; Kang, S.W.; Kim, J.-H.; Nagar, H.; Sabuncu, M.; Margolis, D.J.A.; Kim, C.K. The Role of AI in Prostate MRI Quality and Interpretation: Opportunities and Challenges. *Eur. J. Radiol.* **2023**, *165*, 110887. [CrossRef]
7. Turkbey, B.; Haider, M.A. Artificial Intelligence for Automated Cancer Detection on Prostate MRI: Opportunities and Ongoing Challenges, from the AJR Special Series on AI Applications. *AJR Am. J. Roentgenol.* **2022**, *219*, 188–194. [CrossRef]
8. Nakamae, Y.; Deguchi, R.; Nemoto, M.; Kimura, Y.; Yamashita, S.; Kohjimoto, Y.; Hara, I. AI Prediction of Extracorporeal Shock Wave Lithotripsy Outcomes for Ureteral Stones by Machine Learning-Based Analysis with a Variety of Stone and Patient Characteristics. *Urolithiasis* **2023**, *52*, 9. [CrossRef]
9. Li, J.-W.; Sheng, D.-L.; Chen, J.-G.; You, C.; Liu, S.; Xu, H.-X.; Chang, C. Artificial Intelligence in Breast Imaging: Potentials and Challenges. *Phys. Med. Biol.* **2023**, *68*. [CrossRef]

10. Sheng, K. Artificial Intelligence in Radiotherapy: A Technological Review. *Front. Med.* **2020**, *14*, 431–449. [CrossRef]
11. Plass, M.; Kargl, M.; Kiehl, T.-R.; Regitnig, P.; Geißler, C.; Evans, T.; Zerbe, N.; Carvalho, R.; Holzinger, A.; Müller, H. Explainability and Causability in Digital Pathology. *J. Pathol. Clin. Res.* **2023**, *9*, 251–260. [CrossRef]
12. Comelli, A.; Dahiya, N.; Stefano, A.; Vernuccio, F.; Portoghese, M.; Cutaia, G.; Bruno, A.; Salvaggio, G.; Yezzi, A. Deep Learning-Based Methods for Prostate Segmentation in Magnetic Resonance Imaging. *Appl. Sci.* **2021**, *11*, 782. [CrossRef]
13. Canfora, I.; Cutaia, G.; Marcianò, M.; Calamia, M.; Faraone, R.; Cannella, R.; Benfante, V.; Comelli, A.; Guercio, G.; Giuseppe, L.R.; et al. *A Predictive System to Classify Preoperative Grading of Rectal Cancer Using Radiomics Features*; LNCS Springer: Cham, Switzerland, 2022; pp. 431–440.
14. Roberts, M.; Driggs, D.; Thorpe, M.; Gilbey, J.; Yeung, M.; Ursprung, S.; Aviles-Rivero, A.I.; Etmann, C.; McCague, C.; Beer, L.; et al. Common Pitfalls and Recommendations for Using Machine Learning to Detect and Prognosticate for COVID-19 Using Chest Radiographs and CT Scans. *Nat. Mach. Intell.* **2021**, *3*, 199–217. [CrossRef]
15. Farahat, I.S.; Aladrousy, W.; Elhoseny, M.; Tolba, A.E.; Elmougy, S. CAD System for Intelligent Grading of COVID-19 Severity with Green Computing and Low Carbon Footprint Analysis. *Expert. Syst. Appl.* **2023**, *234*, 121108. [CrossRef]
16. Stefano, A.; Comelli, A. Customized Efficient Neural Network for COVID-19 Infected Region Identification in CT Images. *J. Imaging* **2021**, *7*, 131. [CrossRef] [PubMed]
17. Madabhushi, A.; Lee, G. Image Analysis and Machine Learning in Digital Pathology: Challenges and Opportunities. *Med. Image Anal.* **2016**, *33*, 170–175. [CrossRef] [PubMed]
18. Rizzo, P.C.; Caputo, A.; Maddalena, E.; Caldonazzi, N.; Girolami, I.; Dei Tos, A.P.; Scarpa, A.; Sbaraglia, M.; Brunelli, M.; Gobbo, S.; et al. Digital Pathology World Tour. *Digit. Health* **2023**, *9*, 20552076231194550. [CrossRef]
19. Lin, E.; Fuda, F.; Luu, H.S.; Cox, A.M.; Fang, F.; Feng, J.; Chen, M. Digital Pathology and Artificial Intelligence as the next Chapter in Diagnostic Hematopathology. *Semin. Diagn. Pathol.* **2023**, *40*, 88–94. [CrossRef]
20. Kiran, N.; Sapna, F.; Kiran, F.; Kumar, D.; Raja, F.; Shiwlani, S.; Paladini, A.; Sonam, F.; Bendari, A.; Perkash, R.S.; et al. Digital Pathology: Transforming Diagnosis in the Digital Age. *Cureus* **2023**, *15*, e44620. [CrossRef]
21. Azad, H.; Ahmed, A.; Zafar, I.; Bhutta, M.R.; Rabbani, M.A.; Kc, H.R. X-ray and MRI Correlation of Bone Tumors Using Histopathology as Gold Standard. *Cureus* **2022**, *14*, e27262. [CrossRef]
22. Sonni, I.; Felker, E.R.; Lenis, A.T.; Sisk, A.E.; Bahri, S.; Allen-Auerbach, M.; Armstrong, W.R.; Suvannarerg, V.; Tubtawee, T.; Grogan, T.; et al. Head-to-Head Comparison of 68Ga-PSMA-11 PET/CT and MpMRI with a Histopathology Gold Standard in the Detection, Intraprostatic Localization, and Determination of Local Extension of Primary Prostate Cancer: Results from a Prospective Single-Center Imaging Trial. *J. Nucl. Med.* **2022**, *63*, 847–854. [CrossRef] [PubMed]
23. Bussani, R.; Castrichini, M.; Restivo, L.; Fabris, E.; Porcari, A.; Ferro, F.; Pivetta, A.; Korcova, R.; Cappelletto, C.; Manca, P.; et al. Cardiac Tumors: Diagnosis, Prognosis, and Treatment. *Curr. Cardiol. Rep.* **2020**, *22*, 169. [CrossRef]
24. Baxi, V.; Edwards, R.; Montalto, M.; Saha, S. Digital Pathology and Artificial Intelligence in Translational Medicine and Clinical Practice. *Mod. Pathol.* **2022**, *35*, 23–32. [CrossRef] [PubMed]
25. Pallua, J.D.; Brunner, A.; Zelger, B.; Schirmer, M.; Haybaeck, J. The Future of Pathology Is Digital. *Pathol. Res. Pract.* **2020**, *216*, 153040. [CrossRef] [PubMed]
26. Dawson, H. Digital Pathology—Rising to the Challenge. *Front. Med.* **2022**, *9*, 888896. [CrossRef]
27. Niazi, M.K.K.; Parwani, A.V.; Gurcan, M.N. Digital Pathology and Artificial Intelligence. *Lancet Oncol.* **2019**, *20*, e253–e261. [CrossRef]
28. Hanna, M.G.; Ardon, O.; Reuter, V.E.; Sirintrapun, S.J.; England, C.; Klimstra, D.S.; Hameed, M.R. Integrating Digital Pathology into Clinical Practice. *Mod. Pathol.* **2022**, *35*, 152–164. [CrossRef]
29. Ibrahim, A.; Gamble, P.; Jaroensri, R.; Abdelsamea, M.M.; Mermel, C.H.; Chen, P.-H.C.; Rakha, E.A. Artificial Intelligence in Digital Breast Pathology: Techniques and Applications. *Breast* **2020**, *49*, 267–273. [CrossRef]
30. Rivenson, Y.; Wang, H.; Wei, Z.; de Haan, K.; Zhang, Y.; Wu, Y.; Günaydın, H.; Zuckerman, J.E.; Chong, T.; Sisk, A.E.; et al. Virtual Histological Staining of Unlabelled Tissue-Autofluorescence Images via Deep Learning. *Nat. Biomed. Eng.* **2019**, *3*, 466–477. [CrossRef]
31. Ferreira, D.; Vale, J.; Curado, M.; Polónia, A.; Eloy, C. The Impact of Different Coverslipping Methods in the Quality of the Whole Slide Images Used for Diagnosis in Pathology. *J. Pathol. Inform.* **2022**, *13*, 100098. [CrossRef]
32. Zhang, Y.; Kang, L.; Lo, C.T.K.; Tsang, V.T.C.; Wong, T.T.W. Rapid Slide-Free and Non-Destructive Histological Imaging Using Wide-Field Optical-Sectioning Microscopy. *Biomed. Opt. Express* **2022**, *13*, 2782–2796. [CrossRef]
33. Hesamian, M.H.; Jia, W.; He, X.; Kennedy, P. Deep Learning Techniques for Medical Image Segmentation: Achievements and Challenges. *J. Digit. Imaging* **2019**, *32*, 582–596. [CrossRef]
34. Barisoni, L.; Lafata, K.J.; Hewitt, S.M.; Madabhushi, A.; Balis, U.G.J. Digital Pathology and Computational Image Analysis in Nephropathology. *Nat. Rev. Nephrol.* **2020**, *16*, 669–685. [CrossRef]
35. Al-Thelaya, K.; Gilal, N.U.; Alzubaidi, M.; Majeed, F.; Agus, M.; Schneider, J.; Househ, M. Applications of Discriminative and Deep Learning Feature Extraction Methods for Whole Slide Image Analysis: A Survey. *J. Pathol. Inform.* **2023**, *14*, 100335. [CrossRef]
36. Ivanova, E.; Fayzullin, A.; Grinin, V.; Ermilov, D.; Arutyunyan, A.; Timashev, P.; Shekhter, A. Empowering Renal Cancer Management with AI and Digital Pathology: Pathology, Diagnostics and Prognosis. *Biomedicines* **2023**, *11*, 2875. [CrossRef]

37. Martos, O.; Hoque, M.Z.; Keskinarkaus, A.; Kemi, N.; Näpänkangas, J.; Eskuri, M.; Pohjanen, V.-M.; Kauppila, J.H.; Seppänen, T. Optimized Detection and Segmentation of Nuclei in Gastric Cancer Images Using Stain Normalization and Blurred Artifact Removal. *Pathol. Res. Pract.* **2023**, *248*, 154694. [CrossRef]

38. Kreshuk, A.; Zhang, C. Machine Learning: Advanced Image Segmentation Using Ilastik. *Methods Mol. Biol.* **2019**, *2040*, 449–463. [CrossRef]

39. Priego-Torres, B.M.; Sanchez-Morillo, D.; Fernandez-Granero, M.A.; Garcia-Rojo, M. Automatic Segmentation of Whole-Slide H&E Stained Breast Histopathology Images Using a Deep Convolutional Neural Network Architecture. *Expert. Syst. Appl.* **2020**, *151*, 113387. [CrossRef]

40. Hu, Y.; Yu, J.; Cui, X.; Zhang, Z.; Li, Q.; Guo, W.; Zhao, C.; Chen, X.; Meng, M.; Li, Y.; et al. Combination Usage of AdipoCount and Image-Pro Plus/ImageJ Software for Quantification of Adipocyte Sizes. *Front. Endocrinol.* **2021**, *12*, 642000. [CrossRef]

41. Dionisio, F.C.F.; Oliveira, L.S.; de Andrade Hernandes, M.; Engel, E.E.; de Azevedo-Marques, P.M.; Nogueira-Barbosa, M.H. Manual versus Semiautomatic Segmentation of Soft-Tissue Sarcomas on Magnetic Resonance Imaging: Evaluation of Similarity and Comparison of Segmentation Times. *Radiol. Bras.* **2021**, *54*, 155–164. [CrossRef]

42. Vu, Q.D.; Graham, S.; Kurc, T.; To, M.N.N.; Shaban, M.; Qaiser, T.; Koohbanani, N.A.; Khurram, S.A.; Kalpathy-Cramer, J.; Zhao, T.; et al. Methods for Segmentation and Classification of Digital Microscopy Tissue Images. *Front. Bioeng. Biotechnol.* **2019**, *7*, 53. [CrossRef] [PubMed]

43. Cardenas, C.E.; Yang, J.; Anderson, B.M.; Court, L.E.; Brock, K.B. Advances in Auto-Segmentation. *Semin. Radiat. Oncol.* **2019**, *29*, 185–197. [CrossRef]

44. Comelli, A.; Stefano, A.; Bignardi, S.; Coronnello, C.; Russo, G.; Sabini, M.G.; Ippolito, M.; Yezzi, A. *Tissue Classification to Support Local Active Delineation of Brain Tumors*; CCIS Springer: Cham, Switzerland, 2020; pp. 3–14.

45. Peikari, M.; Salama, S.; Nofech-Mozes, S.; Martel, A.L. A Cluster-Then-Label Semi-Supervised Learning Approach for Pathology Image Classification. *Sci. Rep.* **2018**, *8*, 7193. [CrossRef] [PubMed]

46. Irshad, H.; Veillard, A.; Roux, L.; Racoceanu, D. Methods for Nuclei Detection, Segmentation, and Classification in Digital Histopathology: A Review—Current Status and Future Potential. *IEEE Rev. Biomed. Eng.* **2014**, *7*, 97–114. [CrossRef]

47. Hermsen, M.; de Bel, T.; den Boer, M.; Steenbergen, E.J.; Kers, J.; Florquin, S.; Roelofs, J.J.T.H.; Stegall, M.D.; Alexander, M.P.; Smith, B.H.; et al. Deep Learning-Based Histopathologic Assessment of Kidney Tissue. *J. Am. Soc. Nephrol.* **2019**, *30*, 1968–1979. [CrossRef]

48. Song, Y.; Cisternino, F.; Mekke, J.M.; de Borst, G.J.; de Kleijn, D.P.V.; Pasterkamp, G.; Vink, A.; Glastonbury, C.A.; van der Laan, S.W.; Miller, C.L. An Automatic Entropy Method to Efficiently Mask Histology Whole-Slide Images. *Sci. Rep.* **2023**, *13*, 4321. [CrossRef]

49. Le, D.C.; Chinnasarn, K.; Chansangrat, J.; Keeratibharat, N.; Horkaew, P. Semi-Automatic Liver Segmentation Based on Probabilistic Models and Anatomical Constraints. *Sci. Rep.* **2021**, *11*, 6106. [CrossRef]

50. Waisman, A.; Norris, A.M.; Elías Costa, M.; Kopinke, D. Automatic and Unbiased Segmentation and Quantification of Myofibers in Skeletal Muscle. *Sci. Rep.* **2021**, *11*, 11793. [CrossRef]

51. Encarnacion-Rivera, L.; Foltz, S.; Hartzell, H.C.; Choo, H. Myosoft: An Automated Muscle Histology Analysis Tool Using Machine Learning Algorithm Utilizing FIJI/ImageJ Software. *PLoS ONE* **2020**, *15*, e0229041. [CrossRef]

52. Graham, S.; Vu, Q.D.; Raza, S.E.A.; Azam, A.; Tsang, Y.W.; Kwak, J.T.; Rajpoot, N. Hover-Net: Simultaneous Segmentation and Classification of Nuclei in Multi-Tissue Histology Images. *Med. Image Anal.* **2019**, *58*, 101563. [CrossRef]

53. Muñoz-Aguirre, M.; Ntasis, V.F.; Rojas, S.; Guigó, R. PyHIST: A Histological Image Segmentation Tool. *PLoS Comput. Biol.* **2020**, *16*, e1008349. [CrossRef]

54. Jahn, S.W.; Plass, M.; Moinfar, F. Digital Pathology: Advantages, Limitations and Emerging Perspectives. *J. Clin. Med.* **2020**, *9*, 3697. [CrossRef] [PubMed]

55. Alzoubi, I.; Bao, G.; Zheng, Y.; Wang, X.; Graeber, M.B. Artificial Intelligence Techniques for Neuropathological Diagnostics and Research. *Neuropathology* **2023**, *43*, 277–296. [CrossRef]

56. McQuin, C.; Goodman, A.; Chernyshev, V.; Kamentsky, L.; Cimini, B.A.; Karhohs, K.W.; Doan, M.; Ding, L.; Rafelski, S.M.; Thirstrup, D.; et al. CellProfiler 3.0: Next-Generation Image Processing for Biology. *PLoS Biol.* **2018**, *16*, e2005970. [CrossRef] [PubMed]

57. Schindelin, J.; Arganda-Carreras, I.; Frise, E.; Kaynig, V.; Longair, M.; Pietzsch, T.; Preibisch, S.; Rueden, C.; Saalfeld, S.; Schmid, B.; et al. Fiji: An Open-Source Platform for Biological-Image Analysis. *Nat. Methods* **2012**, *9*, 676–682. [CrossRef] [PubMed]

58. Schneider, C.A.; Rasband, W.S.; Eliceiri, K.W. NIH Image to ImageJ: 25 Years of Image Analysis. *Nat. Methods* **2012**, *9*, 671–675. [CrossRef]

59. ImageJ. Available online: https://imagej.net/ij/index.html (accessed on 25 September 2023).

60. Gerst, R.; Cseresnyés, Z.; Figge, M.T. JIPipe: Visual Batch Processing for ImageJ. *Nat. Methods* **2023**, *20*, 168–169. [CrossRef]

61. Mayeuf-Louchart, A.; Hardy, D.; Thorel, Q.; Roux, P.; Gueniot, L.; Briand, D.; Mazeraud, A.; Bouglé, A.; Shorte, S.L.; Staels, B.; et al. MuscleJ: A High-Content Analysis Method to Study Skeletal Muscle with a New Fiji Tool. *Skelet. Muscle* **2018**, *8*, 25. [CrossRef]

62. Zhi, X.; Wang, J.; Lu, P.; Jia, J.; Shen, H.-B.; Ning, G. AdipoCount: A New Software for Automatic Adipocyte Counting. *Front. Physiol.* **2018**, *9*, 85. [CrossRef]

63. Malhan, D.; Muelke, M.; Rosch, S.; Schaefer, A.B.; Merboth, F.; Weisweiler, D.; Heiss, C.; Arganda-Carreras, I.; El Khassawna, T. An Optimized Approach to Perform Bone Histomorphometry. *Front. Endocrinol.* **2018**, *9*, 666. [CrossRef]

64. Tyagi, S.; Beqollari, D.; Lee, C.S.; Walker, L.A.; Bannister, R.A. Semi-Automated Analysis of Mouse Skeletal Muscle Morphology and Fiber-Type Composition. *J. Vis. Exp.* **2017**, e56024. [CrossRef]

65. Wang, A.Y.; Sharma, V.; Saini, H.; Tingen, J.N.; Flores, A.; Liu, D.; Safain, M.G.; Kryzanski, J.; McPhail, E.D.; Arkun, K.; et al. Machine Learning Quantification of Amyloid Deposits in Histological Images of Ligamentum Flavum. *J. Pathol. Inform.* **2022**, *13*, 100013. [CrossRef] [PubMed]

66. Kanuri, N.; Abdelkarim, A.Z.; Rathore, S.A. Trainable WEKA (Waikato Environment for Knowledge Analysis) Segmentation Tool: Machine-Learning-Enabled Segmentation on Features of Panoramic Radiographs. *Cureus* **2022**, *14*, e21777. [CrossRef] [PubMed]

67. Trainable Weka Segmentation. Available online: https://imagej.net/plugins/tws/ (accessed on 25 September 2023).

68. Babcock, L.W.; Hanna, A.D.; Agha, N.H.; Hamilton, S.L. MyoSight-Semi-Automated Image Analysis of Skeletal Muscle Cross Sections. *Skelet. Muscle* **2020**, *10*, 33. [CrossRef]

69. GitHub—LyleBabcock/MyoSight: Semi-Automated Image Analysis of Skeletal Muscle Cross Sections. Available online: https://github.com/LyleBabcock/MyoSight (accessed on 25 September 2023).

70. Dimitriou, N.; Arandjelović, O.; Caie, P.D. Deep Learning for Whole Slide Image Analysis: An Overview. *Front. Med.* **2019**, *6*, 264. [CrossRef]

71. Lau, Y.S.; Xu, L.; Gao, Y.; Han, R. Automated Muscle Histopathology Analysis Using CellProfiler. *Skelet. Muscle* **2018**, *8*, 32. [CrossRef]

72. Adiposoft. Available online: http://imagej.net/Adiposoft (accessed on 25 September 2023).

73. Galarraga, M.; Campión, J.; Muñoz-Barrutia, A.; Boqué, N.; Moreno, H.; Martínez, J.A.; Milagro, F.; Ortiz-de-Solórzano, C. Adiposoft: Automated Software for the Analysis of White Adipose Tissue Cellularity in Histological Sections. *J. Lipid Res.* **2012**, *53*, 2791–2796. [CrossRef]

74. AdipoCount: Cell Counting System. Available online: http://www.csbio.sjtu.edu.cn/bioinf/AdipoCount/ (accessed on 25 September 2023).

75. Stirling, D.R.; Swain-Bowden, M.J.; Lucas, A.M.; Carpenter, A.E.; Cimini, B.A.; Goodman, A. CellProfiler 4: Improvements in Speed, Utility and Usability. *BMC Bioinform.* **2021**, *22*, 433. [CrossRef]

76. Kamentsky, L.; Jones, T.R.; Fraser, A.; Bray, M.-A.; Logan, D.J.; Madden, K.L.; Ljosa, V.; Rueden, C.; Eliceiri, K.W.; Carpenter, A.E. Improved Structure, Function and Compatibility for CellProfiler: Modular High-Throughput Image Analysis Software. *Bioinformatics* **2011**, *27*, 1179–1180. [CrossRef]

77. Dobson, E.T.A.; Cimini, B.; Klemm, A.H.; Wählby, C.; Carpenter, A.E.; Eliceiri, K.W. ImageJ and CellProfiler: Complements in Open-Source Bioimage Analysis. *Curr. Protoc.* **2021**, *1*, e89. [CrossRef]

78. CellProfiler. Available online: https://cellprofiler.org/ (accessed on 25 September 2023).

79. Sanz, G.; Martínez-Aranda, L.M.; Tesch, P.A.; Fernandez-Gonzalo, R.; Lundberg, T.R. Muscle2View, a CellProfiler Pipeline for Detection of the Capillary-to-Muscle Fiber Interface and High-Content Quantification of Fiber Type-Specific Histology. *J. Appl. Physiol. (1985)* **2019**, *127*, 1698–1709. [CrossRef]

80. Supported Formats—Bio-Formats 5.7.0 Documentation. Available online: https://docs.openmicroscopy.org/bio-formats/5.7.0/supported-formats.html (accessed on 25 September 2023).

81. Berg, S.; Kutra, D.; Kroeger, T.; Straehle, C.N.; Kausler, B.X.; Haubold, C.; Schiegg, M.; Ales, J.; Beier, T.; Rudy, M.; et al. Ilastik: Interactive Machine Learning for (Bio)Image Analysis. *Nat. Methods* **2019**, *16*, 1226–1232. [CrossRef]

82. Ilastik—Ilastik. Available online: https://www.ilastik.org/ (accessed on 25 September 2023).

83. Ilastik—Data Selection. Available online: https://www.ilastik.org/documentation/basics/dataselection#formats (accessed on 25 September 2023).

84. Fischer, C.A.; Besora-Casals, L.; Rolland, S.G.; Haeussler, S.; Singh, K.; Duchen, M.; Conradt, B.; Marr, C. MitoSegNet: Easy-to-Use Deep Learning Segmentation for Analyzing Mitochondrial Morphology. *iScience* **2020**, *23*, 101601. [CrossRef]

85. Yates, S.C.; Groeneboom, N.E.; Coello, C.; Lichtenthaler, S.F.; Kuhn, P.-H.; Demuth, H.-U.; Hartlage-Rübsamen, M.; Roßner, S.; Leergaard, T.; Kreshuk, A.; et al. QUINT: Workflow for Quantification and Spatial Analysis of Features in Histological Images From Rodent Brain. *Front. Neuroinform.* **2019**, *13*, 75. [CrossRef]

86. Rojas-Moraleda, R.; Xiong, W.; Halama, N.; Breitkopf-Heinlein, K.; Dooley, S.; Salinas, L.; Heermann, D.W.; Valous, N.A. Robust Detection and Segmentation of Cell Nuclei in Biomedical Images Based on a Computational Topology Framework. *Med. Image Anal.* **2017**, *38*, 90–103. [CrossRef]

87. Bankhead, P.; Loughrey, M.B.; Fernández, J.A.; Dombrowski, Y.; McArt, D.G.; Dunne, P.D.; McQuaid, S.; Gray, R.T.; Murray, L.J.; Coleman, H.G.; et al. QuPath: Open Source Software for Digital Pathology Image Analysis. *Sci. Rep.* **2017**, *7*, 16878. [CrossRef]

88. What is QuPath? Available online: https://qupath.readthedocs.io/en/0.4/docs/intro/about.html (accessed on 25 September 2023).

89. Supported Image Formats—QuPath 0.4.4 Documentation. Available online: https://qupath.readthedocs.io/en/0.4/docs/intro/formats.html (accessed on 25 September 2023).

90. Bouteldja, N.; Klinkhammer, B.M.; Bülow, R.D.; Droste, P.; Otten, S.W.; Freifrau von Stillfried, S.; Moellmann, J.; Sheehan, S.M.; Korstanje, R.; Menzel, S.; et al. Deep Learning-Based Segmentation and Quantification in Experimental Kidney Histopathology. *J. Am. Soc. Nephrol.* **2021**, *32*, 52–68. [CrossRef]

91. Salvi, M.; Molinari, F. Multi-Tissue and Multi-Scale Approach for Nuclei Segmentation in H&E Stained Images. *Biomed. Eng. Online* **2018**, *17*, 89. [CrossRef]

92. Wills, J.W.; Robertson, J.; Summers, H.D.; Miniter, M.; Barnes, C.; Hewitt, R.E.; Keita, Å.V.; Söderholm, J.D.; Rees, P.; Powell, J.J. Image-Based Cell Profiling Enables Quantitative Tissue Microscopy in Gastroenterology. *Cytometry A* **2020**, *97*, 1222–1237. [CrossRef] [PubMed]

93. Cuadros Linares, O.; Aurea Soriano-Vargas, A.; Faical, B.S.; Hamann, B.; Fabro, A.T.; Traina, A.J.M. Efficient Segmentation of Cell Nuclei in Histopathological Images. In Proceedings of the 2020 IEEE 33rd International Symposium on Computer-Based Medical Systems (CBMS), Rochester, MN, USA, 28–30 July 2020; pp. 47–52.

94. Reinbigler, M.; Cosette, J.; Guesmia, Z.; Jimenez, S.; Fetita, C.; Brunet, E.; Stockholm, D. Artificial Intelligence Workflow Quantifying Muscle Features on Hematoxylin-Eosin Stained Sections Reveals Dystrophic Phenotype Amelioration upon Treatment. *Sci. Rep.* **2022**, *12*, 19913. [CrossRef] [PubMed]

95. Israeli, D.; Cosette, J.; Corre, G.; Amor, F.; Poupiot, J.; Stockholm, D.; Montus, M.; Gjata, B.; Richard, I. An AAV-SGCG Dose-Response Study in a γ-Sarcoglycanopathy Mouse Model in the Context of Mechanical Stress. *Mol. Ther. Methods Clin. Dev.* **2019**, *13*, 494–502. [CrossRef]

96. Graham, S.; Rajpoot, N.M. SAMS-NET: Stain-Aware Multi-Scale Network for Instance-Based Nuclei Segmentation in Histology Images. In Proceedings of the 2018 IEEE 15th International Symposium on Biomedical Imaging (ISBI 2018), Washington, DC, USA, 4–7 April 2018; pp. 590–594.

97. Azevedo Tosta, T.A.; Neves, L.A.; do Nascimento, M.Z. Segmentation Methods of H&E-Stained Histological Images of Lymphoma: A Review. *Inform. Med. Unlocked* **2017**, *9*, 35–43. [CrossRef]

98. Lee, K.; Lockhart, J.H.; Xie, M.; Chaudhary, R.; Slebos, R.J.C.; Flores, E.R.; Chung, C.H.; Tan, A.C. Deep Learning of Histopathology Images at the Single Cell Level. *Front. Artif. Intell.* **2021**, *4*, 754641. [CrossRef]

99. Paulik, R.; Micsik, T.; Kiszler, G.; Kaszál, P.; Székely, J.; Paulik, N.; Várhalmi, E.; Prémusz, V.; Krenács, T.; Molnár, B. An Optimized Image Analysis Algorithm for Detecting Nuclear Signals in Digital Whole Slides for Histopathology. *Cytometry A* **2017**, *91*, 595–608. [CrossRef]

100. Kastenschmidt, J.M.; Ellefsen, K.L.; Mannaa, A.H.; Giebel, J.J.; Yahia, R.; Ayer, R.E.; Pham, P.; Rios, R.; Vetrone, S.A.; Mozaffar, T.; et al. QuantiMus: A Machine Learning-Based Approach for High Precision Analysis of Skeletal Muscle Morphology. *Front. Physiol.* **2019**, *10*, 1416. [CrossRef]

101. Apaolaza, P.S.; Petropoulou, P.-I.; Rodriguez-Calvo, T. Whole-Slide Image Analysis of Human Pancreas Samples to Elucidate the Immunopathogenesis of Type 1 Diabetes Using the QuPath Software. *Front. Mol. Biosci.* **2021**, *8*, 689799. [CrossRef]

102. Arrigoni, C.; Petta, D.; Bersini, S.; Mironov, V.; Candrian, C.; Moretti, M. Engineering Complex Muscle-Tissue Interfaces through Microfabrication. *Biofabrication* **2019**, *11*, 032004. [CrossRef]

103. Hussain, Y.; Miller, S. Other Myopathies. *Neurol. Clin.* **2020**, *38*, 619–635. [CrossRef] [PubMed]

104. Duan, D.; Goemans, N.; Takeda, S.; Mercuri, E.; Aartsma-Rus, A. Duchenne Muscular Dystrophy. *Nat. Rev. Dis. Primers* **2021**, *7*, 13. [CrossRef] [PubMed]

105. Mukund, K.; Subramaniam, S. Skeletal Muscle: A Review of Molecular Structure and Function, in Health and Disease. *Wiley Interdiscip. Rev. Syst. Biol. Med.* **2020**, *12*, e1462. [CrossRef] [PubMed]

106. Ohlendieck, K.; Swandulla, D. Complexity of Skeletal Muscle Degeneration: Multi-Systems Pathophysiology and Organ Crosstalk in Dystrophinopathy. *Pflüg. Arch.* **2021**, *473*, 1813–1839. [CrossRef]

107. Laghi, V.; Ricci, V.; De Santa, F.; Torcinaro, A. A User-Friendly Approach for Routine Histopathological and Morphometric Analysis of Skeletal Muscle Using CellProfiler Software. *Diagnostics* **2022**, *12*, 561. [CrossRef]

108. Reyes-Fernandez, P.C.; Periou, B.; Decrouy, X.; Relaix, F.; Authier, F.J. Automated Image-Analysis Method for the Quantification of Fiber Morphometry and Fiber Type Population in Human Skeletal Muscle. *Skelet. Muscle* **2019**, *9*, 15. [CrossRef] [PubMed]

109. Radi, Z.A. Kidney Pathophysiology, Toxicology, and Drug-Induced Injury in Drug Development. *Int. J. Toxicol.* **2019**, *38*, 215–227. [CrossRef]

110. Firsov, D.; Bonny, O. Circadian Rhythms and the Kidney. *Nat. Rev. Nephrol.* **2018**, *14*, 626–635. [CrossRef] [PubMed]

111. Nicolas, N.; Nicolas, N.; Roux, E. Computational Identification and 3D Morphological Characterization of Renal Glomeruli in Optically Cleared Murine Kidneys. *Sensors* **2021**, *21*, 7440. [CrossRef]

112. Zaza, G.; Cucchiari, D.; Becker, J.U.; de Vries, A.P.J.; Eccher, A.; Florquin, S.; Kers, J.; Rabant, M.; Rossini, M.; Pengel, L.; et al. European Society for Organ Transplantation (ESOT)-TLJ 3.0 Consensus on Histopathological Analysis of Pre-Implantation Donor Kidney Biopsy: Redefining the Role in the Process of Graft Assessment. *Transpl. Int.* **2023**, *36*, 11410. [CrossRef] [PubMed]

113. Girolami, I.; Pantanowitz, L.; Marletta, S.; Hermsen, M.; van der Laak, J.; Munari, E.; Furian, L.; Vistoli, F.; Zaza, G.; Cardillo, M.; et al. Artificial Intelligence Applications for Pre-Implantation Kidney Biopsy Pathology Practice: A Systematic Review. *J. Nephrol.* **2022**, *35*, 1801–1808. [CrossRef]

114. Cazzaniga, G.; Rossi, M.; Eccher, A.; Girolami, I.; L'Imperio, V.; Van Nguyen, H.; Becker, J.U.; Bueno García, M.G.; Sbaraglia, M.; Dei Tos, A.P.; et al. Time for a Full Digital Approach in Nephropathology: A Systematic Review of Current Artificial Intelligence Applications and Future Directions. *J. Nephrol.* **2023**. [CrossRef]

115. Jayapandian, C.P.; Chen, Y.; Janowczyk, A.R.; Palmer, M.B.; Cassol, C.A.; Sekulic, M.; Hodgin, J.B.; Zee, J.; Hewitt, S.M.; O'Toole, J.; et al. Development and Evaluation of Deep Learning-Based Segmentation of Histologic Structures in the Kidney Cortex with Multiple Histologic Stains. *Kidney Int.* **2021**, *99*, 86–101. [CrossRef]

116. Bueno, G.; Fernandez-Carrobles, M.M.; Gonzalez-Lopez, L.; Deniz, O. Glomerulosclerosis Identification in Whole Slide Images Using Semantic Segmentation. *Comput. Methods Programs Biomed.* **2020**, *184*, 105273. [CrossRef] [PubMed]

117. Li, X.; Davis, R.C.; Xu, Y.; Wang, Z.; Souma, N.; Sotolongo, G.; Bell, J.; Ellis, M.; Howell, D.; Shen, X.; et al. Deep Learning Segmentation of Glomeruli on Kidney Donor Frozen Sections. *J. Med. Imaging* **2021**, *8*, 067501. [CrossRef] [PubMed]

118. Singh Samant, S.; Chauhan, A.; Dn, J.; Singh, V. Glomerulus Detection Using Segmentation Neural Networks. *J. Digit. Imaging* **2023**, *36*, 1633–1642. [CrossRef]

119. Dimitri, G.M.; Andreini, P.; Bonechi, S.; Bianchini, M.; Mecocci, A.; Scarselli, F.; Zacchi, A.; Garosi, G.; Marcuzzo, T.; Tripodi, S.A. Deep Learning Approaches for the Segmentation of Glomeruli in Kidney Histopathological Images. *Mathematics* **2022**, *10*, 1934. [CrossRef]

120. Sheehan, S.M.; Korstanje, R. Automatic Glomerular Identification and Quantification of Histological Phenotypes Using Image Analysis and Machine Learning. *Am. J. Physiol. Ren. Physiol.* **2018**, *315*, F1644–F1651. [CrossRef] [PubMed]

121. Komura, D.; Onoyama, T.; Shinbo, K.; Odaka, H.; Hayakawa, M.; Ochi, M.; Herdiantoputri, R.R.; Endo, H.; Katoh, H.; Ikeda, T.; et al. Restaining-Based Annotation for Cancer Histology Segmentation to Overcome Annotation-Related Limitations among Pathologists. *Patterns* **2023**, *4*, 100688. [CrossRef]

122. Wilkinson, L.; Gathani, T. Understanding Breast Cancer as a Global Health Concern. *Br. J. Radiol.* **2022**, *95*, 20211033. [CrossRef]

123. Sechopoulos, I.; Teuwen, J.; Mann, R. Artificial Intelligence for Breast Cancer Detection in Mammography and Digital Breast Tomosynthesis: State of the Art. *Semin. Cancer Biol.* **2021**, *72*, 214–225. [CrossRef]

124. Baker, Q.B.; Abu Qutaish, A. Evaluation of Histopathological Images Segmentation Techniques for Breast Cancer Detection. In Proceedings of the 2021 12th International Conference on Information and Communication Systems (ICICS), Valencia, Spain, 24 May 2021; pp. 134–139.

125. Roulot, A.; Héquet, D.; Guinebretière, J.-M.; Vincent-Salomon, A.; Lerebours, F.; Dubot, C.; Rouzier, R. Tumoral Heterogeneity of Breast Cancer. *Ann. Biol. Clin.* **2016**, *74*, 653–660. [CrossRef]

126. Cammarata, F.P.; Forte, G.I.; Broggi, G.; Bravatà, V.; Minafra, L.; Pisciotta, P.; Calvaruso, M.; Tringali, R.; Tomasello, B.; Torrisi, F.; et al. Molecular Investigation on a Triple Negative Breast Cancer Xenograft Model Exposed to Proton Beams. *Int. J. Mol. Sci.* **2020**, *21*, 6337. [CrossRef]

127. Millar, E.K.; Browne, L.H.; Beretov, J.; Lee, K.; Lynch, J.; Swarbrick, A.; Graham, P.H. Tumour Stroma Ratio Assessment Using Digital Image Analysis Predicts Survival in Triple Negative and Luminal Breast Cancer. *Cancers* **2020**, *12*, 3749. [CrossRef] [PubMed]

128. Juppet, Q.; De Martino, F.; Marcandalli, E.; Weigert, M.; Burri, O.; Unser, M.; Brisken, C.; Sage, D. Deep Learning Enables Individual Xenograft Cell Classification in Histological Images by Analysis of Contextual Features. *J. Mammary Gland. Biol. Neoplasia* **2021**, *26*, 101–112. [CrossRef]

129. Sikpa, D.; Fouquet, J.P.; Lebel, R.; Diamandis, P.; Richer, M.; Lepage, M. Automated Detection and Quantification of Breast Cancer Brain Metastases in an Animal Model Using Democratized Machine Learning Tools. *Sci. Rep.* **2019**, *9*, 17333. [CrossRef] [PubMed]

130. Berben, L.; Wildiers, H.; Marcelis, L.; Antoranz, A.; Bosisio, F.; Hatse, S.; Floris, G. Computerised Scoring Protocol for Identification and Quantification of Different Immune Cell Populations in Breast Tumour Regions by the Use of QuPath Software. *Histopathology* **2020**, *77*, 79–91. [CrossRef]

131. Torrisi, F.; D'Aprile, S.; Denaro, S.; Pavone, A.M.; Alberghina, C.; Zappalà, A.; Giuffrida, R.; Salvatorelli, L.; Broggi, G.; Magro, G.G.; et al. Epigenetics and Metabolism Reprogramming Interplay into Glioblastoma: Novel Insights on Immunosuppressive Mechanisms. *Antioxidants* **2023**, *12*, 220. [CrossRef]

132. Torrisi, F.; Alberghina, C.; D'Aprile, S.; Pavone, A.M.; Longhitano, L.; Giallongo, S.; Tibullo, D.; Di Rosa, M.; Zappalà, A.; Cammarata, F.P.; et al. The Hallmarks of Glioblastoma: Heterogeneity, Intercellular Crosstalk and Molecular Signature of Invasiveness and Progression. *Biomedicines* **2022**, *10*, 806. [CrossRef]

133. Cammarata, F.P.; Torrisi, F.; Vicario, N.; Bravatà, V.; Stefano, A.; Salvatorelli, L.; D'Aprile, S.; Giustetto, P.; Forte, G.I.; Minafra, L.; et al. Proton Boron Capture Therapy (PBCT) Induces Cell Death and Mitophagy in a Heterotopic Glioblastoma Model. *Commun. Biol.* **2023**, *6*, 388. [CrossRef]

134. Wang, L.; Jung, J.; Babikir, H.; Shamardani, K.; Jain, S.; Feng, X.; Gupta, N.; Rosi, S.; Chang, S.; Raleigh, D.; et al. A Single-Cell Atlas of Glioblastoma Evolution under Therapy Reveals Cell-Intrinsic and Cell-Extrinsic Therapeutic Targets. *Nat. Cancer* **2022**, *3*, 1534–1552. [CrossRef] [PubMed]

135. Brancato, V.; Cavaliere, C.; Garbino, N.; Isgrò, F.; Salvatore, M.; Aiello, M. The Relationship between Radiomics and Pathomics in Glioblastoma Patients: Preliminary Results from a Cross-Scale Association Study. *Front. Oncol.* **2022**, *12*, 1005805. [CrossRef]

136. Eidel, O.; Neumann, J.-O.; Burth, S.; Kieslich, P.J.; Jungk, C.; Sahm, F.; Kickingereder, P.; Kiening, K.; Unterberg, A.; Wick, W.; et al. Automatic Analysis of Cellularity in Glioblastoma and Correlation with ADC Using Trajectory Analysis and Automatic Nuclei Counting. *PLoS ONE* **2016**, *11*, e0160250. [CrossRef] [PubMed]

137. Bao, G.; Wang, X.; Xu, R.; Loh, C.; Adeyinka, O.D.; Pieris, D.A.; Cherepanoff, S.; Gracie, G.; Lee, M.; McDonald, K.L.; et al. Patho-Fusion: An Open-Source AI Framework for Recognition of Pathomorphological Features and Mapping of Immunohistochemical Data. *Cancers* **2021**, *13*, 617. [CrossRef] [PubMed]

138. Zygulska, A.L.; Pierzchalski, P. Novel Diagnostic Biomarkers in Colorectal Cancer. *Int. J. Mol. Sci.* **2022**, *23*, 852. [CrossRef] [PubMed]

139. Xiao, X.; Wang, Z.; Kong, Y.; Lu, H. Deep Learning-Based Morphological Feature Analysis and the Prognostic Association Study in Colon Adenocarcinoma Histopathological Images. *Front. Oncol.* **2023**, *13*, 1081529. [CrossRef] [PubMed]
140. Pasini, G.; Stefano, A.; Russo, G.; Comelli, A.; Marinozzi, F.; Bini, F. Phenotyping the Histopathological Subtypes of Non-Small-Cell Lung Carcinoma: How Beneficial Is Radiomics? *Diagnostics* **2023**, *13*, 1167. [CrossRef] [PubMed]
141. Porter, R.J.; Din, S.; Bankhead, P.; Oniscu, A.; Arends, M.J. QuPath Algorithm Accurately Identifies MLH1-Deficient Inflammatory Bowel Disease-Associated Colorectal Cancers in a Tissue Microarray. *Diagnostics* **2023**, *13*, 1890. [CrossRef]
142. Gorman, C.; Punzo, D.; Octaviano, I.; Pieper, S.; Longabaugh, W.J.R.; Clunie, D.A.; Kikinis, R.; Fedorov, A.Y.; Herrmann, M.D. Interoperable Slide Microscopy Viewer and Annotation Tool for Imaging Data Science and Computational Pathology. *Nat. Commun.* **2023**, *14*, 1572. [CrossRef]
143. Cieslak, C.; Mitteldorf, C.; Krömer-Olbrisch, T.; Kempf, W.; Stadler, R. QuPath Analysis for CD30+ Cutaneous T-Cell Lymphoma. *Am. J. Dermatopathol.* **2023**, *45*, 93–98. [CrossRef]
144. Kandemir, M.; Feuchtinger, A.; Walch, A.; Hamprecht, F.A. Digital Pathology: Multiple Instance Learning Can Detect Barrett's Cancer. In Proceedings of the 2014 IEEE 11th International Symposium on Biomedical Imaging (ISBI), Beijing, China, 29 April–2 May 2014; pp. 1348–1351.
145. Escobar Díaz Guerrero, R.; Carvalho, L.; Bocklitz, T.; Popp, J.; Oliveira, J.L. Software Tools and Platforms in Digital Pathology: A Review for Clinicians and Computer Scientists. *J. Pathol. Inform.* **2022**, *13*, 100103. [CrossRef]
146. Campbell, L.; Kumar, M.; Turner, S. Using CellProfiler to Analyze and Quantify Vascular Morphology. *Methods Mol. Biol.* **2017**, *1544*, 179–189. [CrossRef]
147. Steiner, D.F.; Chen, P.-H.C.; Mermel, C.H. Closing the Translation Gap: AI Applications in Digital Pathology. *Biochim. Biophys. Acta (BBA)-Rev. Cancer* **2021**, *1875*, 188452. [CrossRef]